An Improved C-Band Ocean Surface Emissivity Model at Hurricane-Force Wind Speeds Over a Wide Range of Earth Incidence Angles

Salem Fawwaz El-Nimri, *Student Member, IEEE*, W. Linwood Jones, *Life Fellow, IEEE*, Eric Uhlhorn, *Member, IEEE*, Christopher Ruf, *Fellow, IEEE*, James Johnson, *Senior Member, IEEE*, and Peter Black, *Member, IEEE*

***Abstract*—An improved microwave radiometric ocean surface emissivity model has been developed to support forward radiative transfer modeling of brightness temperature and geophysical retrieval algorithms for the next-generation airborne Hurricane Imaging Radiometer instrument. This physically based C-band emissivity model extends current model capabilities to hurricane-force wind speeds over a wide range of incidence angles. It was primarily developed using brightness temperature observations during hurricanes with coincident high-quality surface-truth wind speeds, which were obtained using the airborne Stepped-Frequency Microwave Radiometer. Also, other ocean emissivity models available through the published literature and the spaceborne WindSat radiometer measurements were used.**

***Index Terms*—Hurricane Imaging Radiometer (HIRAD), hurricane winds, ocean surface emissivity, radiometry, Stepped-Frequency Microwave Radiometer (SFMR).**

I. Introduction

AIRBORNE hurricane surveillance provides crucial real-time measurements that are vital to hurricane forecast warnings issued by the National Oceanic and Atmospheric Administration (NOAA) National Hurricane Center (NHC). NOAA and the U.S. Air Force (USAF) Reserve 53rd Weather Reconnaissance Squadron fly specially equipped "Hurricane Hunter" aircraft into storms of the Caribbean Sea and the Atlantic Ocean that threaten the continental U.S. Data collected by *in situ* and remote sensing instruments are delivered in real time to the NHC to help forecasters predict the intensity of the hurricane and its track. Airborne measurements include the hurricane eye location, the central pressure, and the peak surface wind speed. Of these, the maximum sustained (1-min average) surface wind speed at the 10-m level is of greatest importance because this is the determining factor in the Saffir–Simpson hurricane scale commonly known as the hurricane category. For the past two decades, the airborne Stepped-Frequency Microwave Radiometer (SFMR) has provided real-time measurements of surface wind speed and rain rates in hurricanes [1]. These measurements are crucial because SFMR is the only remote sensor that is capable of providing continuous measurements of surface wind speeds up to and including Category-5 (CAT5) hurricane conditions. Furthermore, since 2006, operational SFMR sensors have been installed on both NOAA WP-3D and USAF WC-130J aircraft.

The Hurricane Imaging Radiometer (HIRAD) is the next-generation version of SFMR, which is developed by the National Aeronautics and Space Administration Marshall Space Flight Center, the NOAA Hurricane Research Division (HRD), the University of Michigan, and the Central Florida Remote Sensing Laboratory (CFRSL). HIRAD is a hybrid design that is both a multifrequency radiometer, similar to SFMR, and a Fourier synthesis imager, similar to the Lightweight Rain Radiometer [2]. It uses synthetic thinned-array interferometric radiometry to synthesize C-band (4–6.6-GHz) ocean brightness temperature (T_b) pixels cross track and real-aperture push-broom imaging along track [3] for retrievals of hurricane surface winds and rain rates over a swath width of approximately three times the aircraft altitude. Extending the nadir-viewing SFMR wind speed retrieval capabilities to HIRAD requires the development of a more general ocean surface emissivity model, which is the subject of this letter.

II. Ocean Emissivity Model Formulation

For HIRAD, the retrieval of hurricane wind speed requires an ocean emissivity model that must accommodate the full range of Earth incidence angles (EIAs) from nadir to $> 60^\circ$ and ocean wind speeds from 10 m/s to CAT5 winds under atmospheric boundary layer stability conditions from neutral to slightly unstable that are typical of most hurricanes. There are many ocean emissivity models available, but unfortunately, none fully satisfies these stringent HIRAD requirements. Because of the limited availability of off-nadir C-band T_b observations in hurricanes and the difficulty of performing new

Manuscript received April 15, 2009; revised July 21, 2009 and November 16, 2009. Date of publication April 12, 2010; date of current version May 7, 2010. This work was supported in part by the Von Braun Center for Science and Innovation, Inc., Huntsville, AL, under Subcontract SUB2006-226, by the Marshall Space Flight Center, National Aeronautics and Space Administration, and by the National Oceanic and Atmospheric Administration in the development of the Hurricane Imaging Radiometer instrument.

S. F. El-Nimri, W. L. Jones, and J. Johnson are with the Central Florida Remote Sensing Laboratory, University of Central Florida, Orlando, FL 32816 USA (e-mail: selnimri@mail.ucf.edu; ljones@ucf.edu; jamesj@mail.ucf.edu).

E. Uhlhorn is with the Hurricane Research Division, Atlantic Oceanographic and Meteorological Laboratory, National Oceanic and Atmospheric Administration, Miami, FL 33149 USA (e-mail: eric.uhlhorn@noaa.gov).

C. Ruf is with the University of Michigan, Ann Arbor, MI 48109 USA (e-mail: cruf@umich.edu).

P. Black is with SAIC, Inc., CA 93940 USA, and also with the Marine Meteorology Division, Naval Research Laboratory, Monterey, CA 93940 USA (e-mail: peter.black@nrlmry.navy.mil).

Color versions of one or more of the figures in this paper are available online at http://ieeexplore.ieee.org.

Digital Object Identifier 10.1109/LGRS.2010.2043814

measurements with associated surface truth, we have developed a hybrid physically based/empirically tuned model, which provides the flexibility of extrapolating ocean emissivity to other regimes where measurements are possible but have not yet been observed.

A. Existing Ocean Emissivity Models

There are three ocean emissivity models, which are applicable to HIRAD. First, the NOAA SFMR emissivity model by Uhlhorn *et al.* [1] is the only model that is capable of estimating ocean emissivity over the full range of wind speeds from 10 to > 70 m/s. This empirical statistical regression model is based upon SFMR C-band T_b measurements in hurricanes that are collocated with 10-m ocean surface wind speed measurements derived from GPS dropwindsondes; however, because this algorithm applies only at nadir, its utility to HIRAD is limited. Second, the model by Stogryn [4] is a physically based approach, with empirical coefficients based on radiometric measurements of foam-covered sea surfaces, which calculates the ocean emissivity for the HIRAD frequencies and EIA range. Unfortunately, this model exhibits unrealistic emissivity saturation at wind speeds > 45 m/s; therefore, significant corrections are required. Third, the emissivity model by Wentz and Meissner [5] has been developed for conical scanning satellite radiometers, but it is limited to a narrow range of EIAs (49°–57°) and for wind speeds < 20 m/s. Thus, because no single model is fully satisfactory, all three ocean emissivity models are used in the development of the new CFRSL HIRAD emissivity model [6].

B. CFRSL Ocean Emissivity Model

This model uses the formulation of Stogryn with modified model coefficients that are tuned to Uhlhorn and Wentz ocean emissivities in their range of applicability and new off-nadir hurricane T_b measurements for SFMR and WindSat. Where empirical data do not exist, the emissivity is constrained to vary smoothly in a monotonic manner and without an inflection point in the first derivative with respect to model parameters (wind speed, EIA, and frequency). Furthermore, to extrapolate model parameters beyond the range of observations, the CFRSL emissivities are constrained to asymptotically approach physically realizable limits. All model coefficients are derived in an iterative manner to provide a weighted least mean squares fit to the empirical T_b data (SFMR and WindSat) and the total ocean emissivities of the Uhlhorn and Wentz models across the model parameter space.

Like Stogryn, the CFRSL ocean surface emissivity $(\varepsilon_{\text{ocean}})$ is modeled as a linear sum of foam $(\varepsilon_{\text{foam}})$ and foam-free seawater $(\varepsilon_{\text{rough}})$ emissivities, according to

$$\varepsilon_{\text{ocean}} = FF \times \varepsilon_{\text{foam}} + (1 - FF) \times \varepsilon_{\text{rough}} \tag{1}$$

where FF is the fractional area coverage by foam. The foam emissivity is modeled as

$$\varepsilon_{\text{foam}} = Q(freq) \times f(U_{10}, EIA) \tag{2}$$

where $Q(freq)$ is the empirical frequency dependence and $f(U_{10}, EIA)$ is the empirical dependence on the 10-m neutral stability wind speed and EIA. Following Stogryn, the foam-free seawater emissivity $(\varepsilon_{\text{rough}})$ is

$$\varepsilon_{\text{rough}} = \varepsilon_{\text{smooth}} + \Delta\varepsilon_{\text{excess}} \tag{3}$$

where $\varepsilon_{\text{smooth}} = (1 - \Gamma)$ is the smooth surface emissivity, Γ is the Fresnel power reflection coefficient, and $\Delta\varepsilon_{\text{excess}}$ is the wind-induced excess emissivity, given by

$$\Delta\varepsilon_{\text{excess}} = g(U_{10}, EIA) \times \frac{\sqrt{freq}}{SST} \tag{4}$$

where SST is the sea surface temperature and $g(U_{10}, EIA)$ is tuned to SFMR off-nadir T_b measurements and the Wentz and Meissner model ocean emissivity.

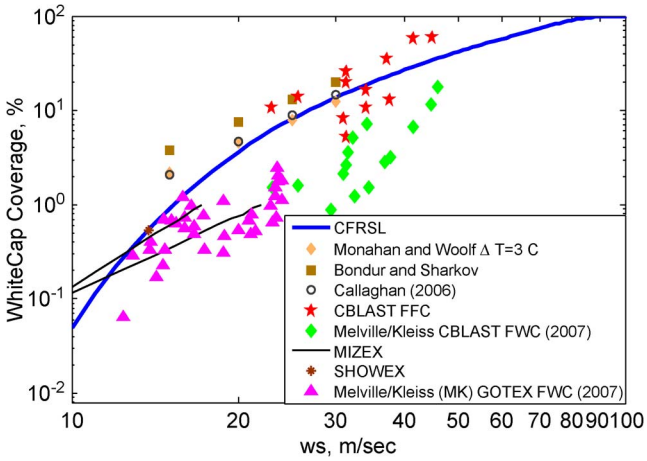

Fig. 1. CFRSL FF parameterization with respect to (solid curve) 10-m oceanic wind speed with empirical observations of percentage of sea foam coverage.

1) Foam Model Coefficient Tuning: At hurricane-force wind speeds, foam emission is the dominant component of the ocean brightness temperature. Sea foam is produced when ocean gravity waves break, which occurs at wind speeds > 7 m/s, and the fractional area foam coverage increases almost exponentially with wind speed (see Fig. 1). At SFMR and HIRAD frequencies (4–6.6 GHz), the emissivity of foam is almost twice that of the rough (foam-free) ocean surface for horizontal polarization (H-pol).

At nadir, the CFRSL model coefficients for foam emissivity and foam fraction (FF) were derived using an iterative procedure to maximize agreement with the Uhlhorn SFMR ocean emissivity model. First, the emissivity of foam was assumed to be only a function of frequency $[Q(freq)]$, so the $f(U_{10}, EIA = 0)$ term in (2) was set equal to unity for all U_{10}. From the Uhlhorn model, the total ocean emissivity at 70 m/s was determined, and the foam-free $(\varepsilon_{\text{rough}})$ contribution was subtracted to yield the foam emissivity. Taking the derivative with respect to frequency yielded the estimate of $Q(freq)$. It should be noted that, according to (4), there is also a frequency dependence of the foam-free $\varepsilon_{\text{rough}}$ that is small. Using a least squares regression of the foam emissivity at the six SFMR frequencies yields

$$Q(freq) = 0.036659 \times freq + 0.57767 \tag{5}$$

where $freq$ has units of gigahertz.

TABLE I
HURRICANES USED IN HIRAD MODEL DEVELOPMENT

Hurricane	Year	max 1-min sustained wind speed	Number of flights
Fabian	2003	120 kt (60 m/s)	3
Frances	2004	115 kt (58 m/s)	6
Katrina	2005	150 kt (75 m/s)	4
Ophelia	2005	65 kt (34 m/s)	4
Rita	2005	155 kt (78 m/s)	5

Next, the dependence of FF on wind speed was derived using the Uhlhorn emissivity model over the dynamic range of 0–70 m/s. In this calculation, Stogryn's $\varepsilon_{\rm rough}$ was used; however, since the function $g(U_{10}, EIA = 0)$ in (4) was allowed to change, the FF was also calculated iteratively

$$FF = \frac{\langle \varepsilon_{\rm SFMR} \rangle_{\rm freq} - \langle \varepsilon_{\rm rough} \rangle_{\rm freq}}{\langle \varepsilon_{\rm foam} \rangle_{\rm freq} - \langle \varepsilon_{\rm rough} \rangle_{\rm freq}} \tag{6}$$

where "$\langle\rangle$" denotes average values. At wind speeds > 70 m/s, FF was modeled to asymptotically approach 100%, as shown in Fig. 1. Also shown are independent measurements from the Coupled Boundary Layer Air–Sea Transfer (CBLAST) experiment [7] of foam fractional coverage (FFC), in the North Atlantic from Callaghan *et al.* [8], Bondur and Skarkov [9], and Monahan and Woolf [10], which compare well with our model. The Melville/Kleiss CBLAST and GOTEX foam whitecap coverage (FWC) were added to Fig. 1 for completeness and to show the difference between FWC and FFC, where FFC is the main interest because it represents the total foam coverage (whitecaps and streaks).

2) Wind Speed and EIA Coefficient Tuning: The HIRAD geometry requires an emissivity model that is applicable from nadir to $> 60^\circ$ over the full range of wind speeds (0–70 m/s). Based upon the findings of Reul and Chapron [11], we model the emissivity of foam in (2) as a function of U_{10} and EIA. The functional form of this dependence was developed empirically using SFMR (airborne) and WindSat (satellite) measurements in several hurricanes with near-simultaneous aircraft underflights providing "surface truth." Radiometric measurements at off-nadir angles were collected at wind speeds greater than 20 m/s, where foam has an appreciable contribution to the total ocean emission.

a) SFMR measurements: This data set comprised brightness temperatures from SFMR flights during the 2003–2005 hurricane seasons (Table I). It included measurements at high wind speeds and off-nadir incidence angles up to 35° for H-pol and vertical polarization (V-pol) that were analyzed to extract the ocean surface emissivity from SFMR brightness temperatures. First, the data were filtered to extract off-nadir measurements during steady aircraft turns, which resulted in a small data set with reduced dynamic range of available wind speeds. This occurred because turns were not performed in the eye wall region (maximum winds) due to safety concerns. Next, the data were examined for radio-frequency interference (RFI) detection, and contaminated SFMR measurements were removed from the data set. Because of onboard C-band radars, RFI was experienced on one or more channels approximately

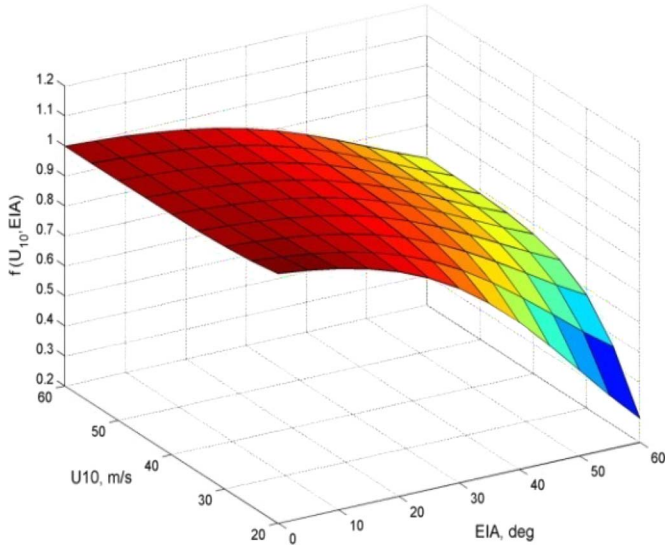

Fig. 2. Foam emissivity dependence $[f(U_{10}, EIA)]$ with respect to U_{10} (in meters per second) and EIA (in degrees) for H-pol.

15%–25% of the time. Fortunately, the RFI was relatively easy to detect by relative comparison among SFMR channels using a T_b threshold.

The next step involved "atmospheric clearing" to remove the atmospheric component of SFMR T_b before estimation of the ocean surface emissivity. For this purpose, radiative transfer calculations were performed using a typical hurricane atmosphere by Frank [12]. Furthermore, the effects of rain (emission and attenuation) were removed using the approach of Uhlhorn *et al.* [1], [13]. Data sets were carefully selected to minimize regions with heavy rain, but typically, rain atmospheric clearing was required. This involved estimating the rain rate along the propagation path using SFMR rain retrievals during level flight before and after the turns. For atmospheric clearing, the rain was assumed to be homogeneous with a 100% antenna beam fill. This is considered to be valid because the SFMR operated at low altitudes (< 2.5 km) and at low bank angles ($< 35^\circ$), which resulted in the line of sight being displaced by < 1.75 km from nadir. Atmospheric clearing typically yielded T_b adjustments of < 5 K [6].

The final data reduction step involved an antenna pattern correction to remove T_b biases caused by the broad SFMR antenna beamwidth (15°–28°). In this procedure, we first calculated the antenna temperature as a weighted average (convolution) of the antenna gain pattern with the Fresnel smooth surface T_b as a function of EIA. Next, the differential between this antenna pattern-weighted T_b and the Fresnel brightness was calculated versus EIA. Finally, this was subtracted from the SFMR measurement to yield the corrected T_b. Typically, this process resulted T_b biases < 4 K (depending on the aircraft roll angle) and yielded an improved estimate of the true brightness temperature at the antenna boresight EIA [6].

b) Satellite measurements: For high EIA (49°–57°), the surface emissivity model by Wentz and Meissner [5] was used to estimate the total ocean emissivity versus wind speed. Wentz and Meissner's results were based upon over one decade of Special Sensor Microwave/Imager and Tropical Rainfall

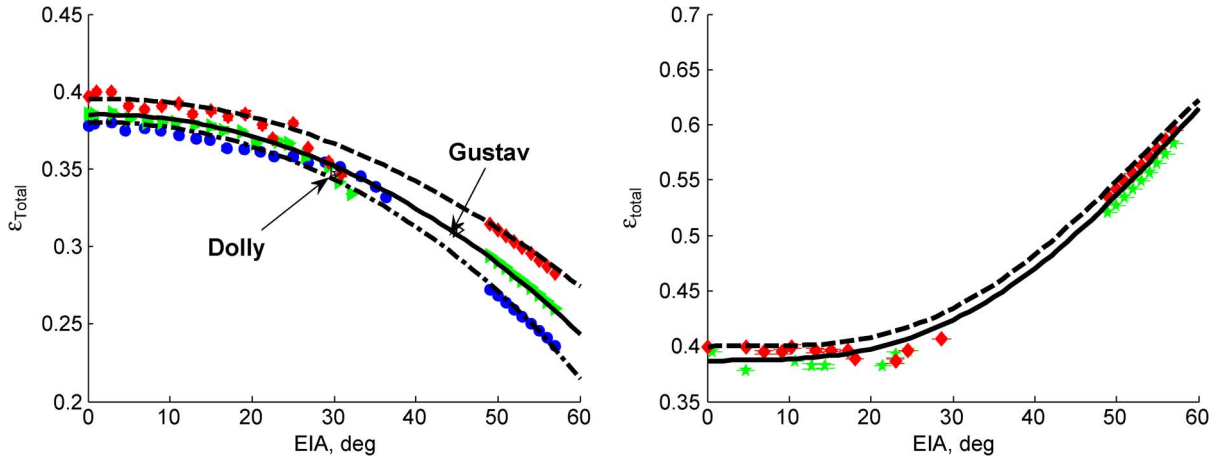

Fig. 3. Total ocean emissivity for (left) H-pol and (right) V-pol for wind speed bins of (○) (5–10 m/s), (∗ and ▶) (10–15 m/s), and (◇) (15–20 m/s), where the vertical bars represent one-standard deviation of the binned average.

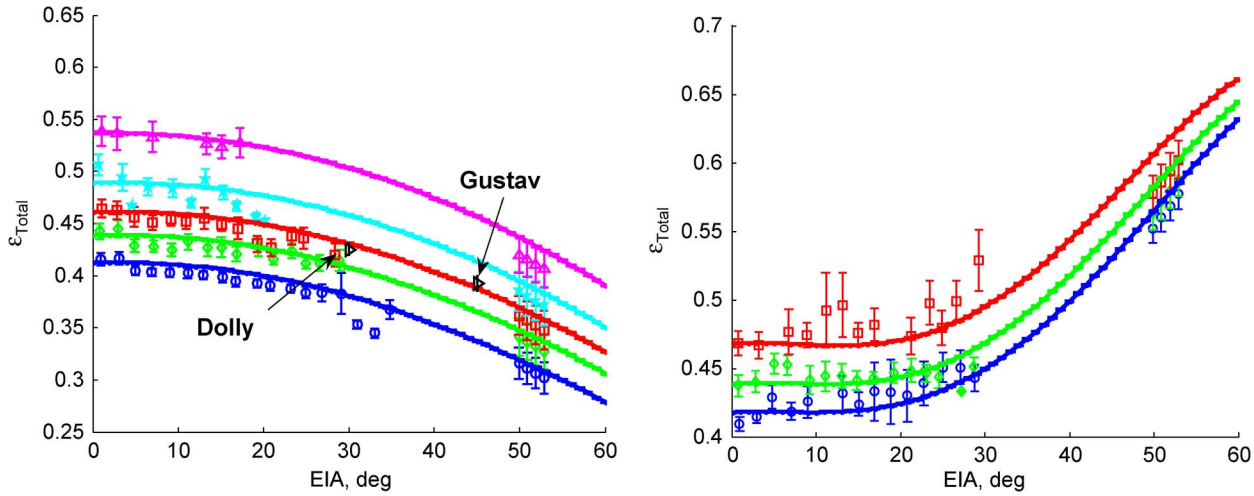

Fig. 4. Total ocean emissivity (left) H-pol and (right) V-pol for wind speed bins of (○) (20–25 m/s), (◇) (25–30 m/s), (□ and ▶) (30–35 m/s), (∗) (35–40 m/s), and ▲ (40–45 m/s), where the vertical bars represent one standard deviation of the binned average.

Measuring Mission Microwave Imager T_b comparisons with *in situ* wind speed measurements on buoys, which were extrapolated to the HIRAD C-band frequencies. The buoy data set only extended to ∼20 m/s; therefore, hurricane observations from the WindSat polarimetric radiometer were used for higher wind speeds.

An analysis of WindSat C-band (6.8 GHz) V- and H-pol T_b in hurricanes by Ruf *et al.* [14] was used to estimate the total ocean emissivity at high wind speeds and EIAs (49°–55°). This study involved satellite radiometer measurements obtained during 2005 hurricanes (Dennis, Rita, and Katrina) and associated high-quality surface wind fields derived from NOAA HRD aircraft underflights with SFMR. Results showed a well-behaved and monotonic increase in the C-band ocean emissivity with surface wind speed provided using NOAA's H*Wind analysis procedure (see [14, Table 1 and Fig. 5]). These data were extrapolated to HIRAD's C-band frequencies (4–6.6 GHz) and were then used subjectively as points of reference at higher EIA ($> 45°$) in a weighted least mean squares sense to derive $f(U_{10}, EIA)$ in (2).

c) Wind speed modeling: Because of the distinct contributions by rough water and foam in (1), modeling of the ocean surface emissivity was broken into two parts: wind speeds $U_{10} \leq 20$ m/s and higher wind speeds. In both cases, measurements from SFMR and satellites were used to estimate our model coefficients using regression analysis, and special care was taken to assure a smooth transition with wind speed.

For wind speeds $5 \leq U_{10} \leq 20$ m/s, the rough-water emissivity term dominates, and both sets (aircraft and satellite) of total ocean emissivities were used to derive $g(U_{10}, EIA)$ in (4). Ocean emissivity values derived from SFMR measurements were binned and averaged with respect to U_{10} (5-m/s bins) and EIA from nadir to 35° (2° bins). For high EIA (49°–57°), the surface emissivity model by Wentz and Meissner [5] was extrapolated to SFMR frequencies and used to provide the ocean emissivity versus wind speed at higher EIA. While the Wentz and Meissner model has not been validated versus wind speed below 10.6 GHz, we feel that uncertainties due to extrapolation to C-band are not dominant over the wind speed range used. The dependence of emissivity on EIA was assumed to be

monotonic from nadir for both polarizations (increasing for V-pol but decreasing for H-pol). For the regression analysis, each binned data point was given an independent weight based on the number of points in that bin and the subjective confidence of these measurements. For V-pol, the number of SFMR observations is significantly less, and the resulting regression fit for the CFRSL emissivity model has much higher residuals. This was particularly true for SFMR measurements between 20° and 30°, which were of lesser quality because of possible errors in the atmospheric clearing for rain effects.

For higher wind speeds ($U_{10} > 20$ m/s), foam becomes the dominant contributor to ocean surface emissivity; and SFMR and WindSat hurricane observations were used to estimate the foam emissivity dependence on wind speed and EIA. The $f(U_{10}, EIA)$ in (2) was derived from a regression analysis using only SFMR data (WindSat data were used subjectively as constraints), and results for H-pol are shown in Fig. 2. Because of spatial averaging over the large antenna footprint (40 km × 60 km), we believe that the WindSat emissivities [14] for both V- and H-pols are progressively underestimated with increasing wind speed.

III. Results

The results shown in Fig. 3 show the total ocean emissivity measurements in the range $5 \leq U_{10} \leq 20$ m/s, where emissivities based upon experimental observations (symbols) were from SFMR (nadir–35°) and Wentz (49°–57°). CFRSL model results (solid lines) are in excellent agreement with these total ocean emissivity values for both polarizations. As discussed previously, the V-pol SFMR total emissivity values have greater deviations from our model between 20° and 30°, but we believe that our model's monotonic dependence on EIA is more consistent with electromagnetic theory than are the SFMR measurements during aircraft banked turns.

The results shown in Fig. 4 compare the CFRSL model with surface emissivity values, derived from SFMR and WindSat, over the wind speed range of 20–45 m/s. For H-pol (left panel), the model (solid lines) exhibits excellent agreement with the SFMR, but the agreement with WindSat is slightly degraded as the wind speed increases. As discussed earlier, we believe that the WindSat emissivities are too low because of spatial averaging over the large antenna footprint. On the other hand, the V-pol comparisons of the CFRSL model with the SFMR and WindSat data exhibit relatively larger differences. As discussed before, we attribute this to the lesser quality of the SFMR and WindSat data.

Finally, two independent SFMR measurements of total ocean emissivity are available from NOAA HRD during the 2008 hurricane season (hurricanes Dolly and Gustav).

In these experiments, the NOAA WP3 aircraft flew consecutive circles at 30° and 45° banks in clear (rain-free) regions with surface wind speeds of 15 m/s (see the Fig. 3 left panel) and 35 m/s (see the Fig. 4 left panel) [15]. Since these measurements were not used in the CFRSL model development, they are shown in Figs. 3 and 4 as points of independent comparison. There is excellent agreement with the CFRSL model for these two high-quality off-nadir emissivity measurements.

IV. Summary and Conclusion

This letter has presented a new microwave (C-band: 4–6.6 GHz) ocean surface emissivity model that has been developed for the airborne HIRAD instrument for hurricane remote sensing applications. This model extends the capability of current ocean emissivity models to a wider range of EIAs (0°–60°), higher wind speeds (0–70 m/s), and for both H- and V-pols. This model has been tuned using available airborne (SFMR) hurricane measurements, an extrapolated spaceborne radiometer emissivity model (Wentz and Meissnen [5]), and WindSat measurements in hurricane conditions. The model exhibits a good fit with low residuals over a wide range of EIAs and wind speeds. Also, the derived relationship for hurricane sea foam parameters with respect to wind speed agrees well with independent FFC observations and foam emissivity measurements in the C-band frequency range. Future improvements are expected once the HIRAD instrument flies in hurricanes during the 2010 season.

References

[1] E. W. Uhlhorn, P. G. Black, J. L. Franklin, and A. S. Goldstein, "Hurricane surface wind measurements from an operational Stepped Frequency Microwave Radiometer," *Mon. Weather Rev.*, vol. 135, no. 9, pp. 3070–3085, Sep. 2007.

[2] C. Ruf and C. Principe, "X-band lightweight rainfall radiometer first light," in *Proc. IEEE IGARSS*, Toulouse, France, Jul. 21–25, 2003, pp. 1701–1703.

[3] C. S. Ruf, R. Amarin, M. C. Bailey, B. Lim, R. Hood, M. James, J. Johnson, L. Jones, V. Rohwedder, and K. Stephens, "The hurricane imaging radiometer—An octave bandwidth synthetic thinned array radiometer," in *Proc. IEEE IGARSS*, Barcelona, Spain, Jul. 23–27, 2007, pp. 231–234.

[4] A. Stogryn, "The apparent temperature of the sea at microwave frequencies," *IEEE Trans. Antennas Propag.*, vol. AP-15, no. 2, pp. 278–286, Mar. 1967.

[5] F. Wentz and T. Meissner, "AMSR Ocean Algorithm," Remote Sens. Syst., Santa Rosa, CA, Tech. Rep. 2, Nov. 2000.

[6] S. F. El-Nimri, "An improved microwave radiative transfer model for ocean emissivity at hurricane force surface wind speed," M.S. thesis, School Elect. Eng. Comput. Sci., Univ. Central Florida, Orlando, FL, 2006.

[7] S. S. Chen, "CBLAST—Hurricane and high-resolution fully coupled atmosphere–wave–ocean models," in *Proc. 10th Wave Hindcasting Workshop*, Oahu, HI, 2007.

[8] A. Callaghan, G. de Leeuw, and L. Cohen, "Observations of oceanic whitecap coverage in the North Atlantic during gale force winds," in *Nucleation and Atmospheric Aerosols*. Galway, Ireland: Springer-Verlag, 2007, pp. 1088–1092.

[9] V. G. Bondur and E. A. Sharkov, "Statistical properties of whitecaps on a rough sea," *Oceanology*, vol. 22, no. 3, pp. 274–279, 1982.

[10] E. Monahan and D. K. Woolf, "Comments on 'Variations of whitecap coverage with wind stress and water temperature'," *J. Phys. Oceanogr.*, vol. 19, no. 5, pp. 706–709, May 1989.

[11] N. Reul and B. Chapron, "A model of sea-foam thickness distribution for passive microwave remote sensing applications," *J. Geophys. Res.*, vol. 108, no. C10, pp. 19.1–19.14, Oct. 2003.

[12] W. M. Frank, "The structure and energetics of the tropical cyclone. I. Storm structure," *Mon. Weather Rev.*, vol. 105, no. 9, pp. 1119–1135, Sep. 1977.

[13] E. W. Uhlhorn and P. G. Black, "Verification of remotely sensed sea surface winds in hurricanes," *J. Atmos. Ocean. Technol.*, vol. 20, no. 1, pp. 100–115, Jan. 2003.

[14] C. S. Ruf, A. M. Mims, and C. C. Hennon, "The dependence of the microwave emissivity of the ocean on hurricane force wind speed," in *Proc. 28th Conf. Hurricanes Trop. Meteorol.*, Orlando, FL, Apr. 28–May 2, 2008.

[15] E. W. Uhlhorn, S. F. El-Nimri, C. S. Ruf, and W. L. Jones, "Sea surface passive microwave measurements at large incidence angle in hurricane conditions," *IEEE Geosci. Remote Sens. Lett.*, to be published.